

DIAGNOSIS AND ON-LINE PARAMETRIC ESTIMATION OF AUTOMOTIVE ELECTRONIC THROTTLE CONTROL SYSTEMS

Bilal Youssef* Mazen Alamir*

* *Laboratoire d'Automatique de Grenoble, UMR 5528
CNRS-INPG-UJF. Saint Martin d'Hères, France. Emails :
bilal.youssef@inpg.fr, mazen.alamir@inpg.fr*

Abstract: In this paper, a recently developed graphical signatures generation tool is used for diagnosis and on-line parametric estimation of automotive electronic throttle control (ETC) system. The underlying diagnosis problem corresponds to variations affecting four system's parameters. It is shown that this diagnosis method enables detection, isolation and parameter estimation even under simultaneous faults occurrence outperforming existing works on the same problem. *Copyright© 2005 IFAC.*

Keywords: Engine management; Modeling; Diagnosis; signature analysis; multiple faults; parameter estimation.

1. INTRODUCTION

Diagnosis of automotive components and subsystems becomes a crucial issue in the automotive industry (Krishnaswami *et al.*, 1995; Conatser *et al.*, 2004; Conatser and Wagner, 2000). Diagnosis includes fault detection and isolation. By fault detection, one means that a faulty behaviour symptoms have been detected while isolation amounts to identify the precise fault configuration leading to these symptoms.

There are several techniques that may be used to perform the above tasks. Diagnosis may be done using dedicated observers (Ding and Guo, 1998). Analytical redundancy can also be used in an algebraic framework in order to detect variations on parameters (Staroswiecki and Comtet-Varga, 2001). Fuzzy logic-based schemes may be invoked through parity equations (Xiang-Fang *et al.*, 2002). Statistical and local approaches based on signal processing and statistical properties monitoring have been proposed (Basseville, 1998)

as well as methods based on the wavelets transformation (Petropol, 2001) that can generically be applied to detect singular behaviors based on the spectral content of the measured signals.

In the present paper, a recently developed (Youssef and Alamir, 2003) signature-based methodology is used to derive a diagnosis tool for the automotive Electronic Throttle Control (**ETC**) device. The signature based methodology proposed in (Youssef and Alamir, 2003) uses a general signature generation algorithm to yield a diagnosis procedure by means of the following three steps : **Step 1: Generating signatures.** In this first step, a family of 2D graphical signatures is generated for nominal and faulty configurations. This is done using the physical simulation model in which variations on the parameters are introduced. Furthermore, several parameterizations of the signature generation tool are used in order to enhance detection and isolation capacity.

Step 2: Signature analysis. In this second step,

the high classification ability of human brain is used to analyse the signatures produced in the first step. The way variations on parameters induce signature deformations is analysed in order to define relevant GEOMETRICAL residuals. This step may invoke the first one in order to produce additional signatures enabling detection and isolation to be performed.

Step 3: Definition of mathematical residuals. Once a relevant set of geometrical residuals is defined in Step 2. A mathematical translation is then performed in order to derive mathematical residuals that can be used in an on-line diagnosis framework.

The above three-steps diagnosis design strategy is applied in this paper to yield a novel diagnosis algorithm for the automotive **ETC** diagnosis problem. This problem has been recently studied by (Conatser *et al.*, 2004) using a parity-based diagnostic strategy. However, while in (Conatser *et al.*, 2004), only single faults are handled and no parameter estimation is performed, the strategy proposed here enables simultaneous faults affecting any combination of 4 parameters to be detected and isolated. Moreover, the estimation of the new parameters configuration is simultaneously obtained.

The paper is organized as follows. The **ETC** system model is presented in section 2 and the diagnosis problem under interest is clearly stated. Section 3 recalls the technique based on graphical signature (Youssef and Alamir, 2003) for the fault detection and isolation of dynamical systems which is used. Application of this methodology to the **ETC** diagnosis problem is presented in section 4. Section 5 shows how one can estimate the values of parameters using an automatic on-line ETC parametric estimation. The paper ends with a conclusion.

2. THE ELECTRONIC THROTTLE CONTROL DIAGNOSIS PROBLEM

The Electronic Throttle Control system **ETC** is used to regulate the inlet airflow rate. This is done by means of a DC servo-motor which controls the throttle plate angle. The **ETC** is integrated into existing engine management systems (manifold, fueling, combustion process, and rotational dynamics). The driver's commands and the throttle position feedback signals are processed by the ETC controller to regulate the servo-motor voltage e_a which controls the angle $\theta \in [0, \pi/2]$ of the **ETC** throttle plate (Huber *et al.*, 1991). Figure 1 shows the electro-mechanical dynamic system scheme (Conatser and Wagner, 2000).

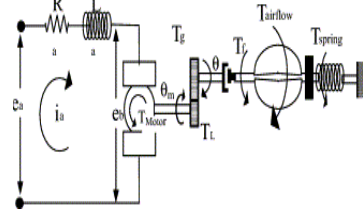


Fig. 1. Mechatronic system diagram for throttle-by-wire

2.1 The system equations

The evolution of the armature current i_a is given by the following differential equation:

$$\frac{di_a}{dt} = \frac{1}{L_a}(-R_a i_a - K_b \frac{d\theta_m}{dt} + e_a) \quad (1)$$

where R_a and L_a are the armature resistance and inductance, respectively. $K_b \frac{d\theta_m}{dt}$ represents the back e.m.f induced by the motor rotation. The throttle body's rotational dynamics may be described by:

$$\frac{d^2\theta}{dt^2} = \frac{1}{N^2 J_m + J_g} \left(-(N^2 b_m + b_t) \frac{d\theta}{dt} + N T_m - T_{sp} - T_a \right)$$

where :

✓ b_m and b_t denote the motor shaft and throttle viscous damping coefficients, respectively.

✓ N is the gear ratio, that is $N = \theta_m / \theta$ (see figure 1)

✓ T_m is the motor torque that is related to the current i_a since $T_m = K_t i_a$.

✓ T_{sp} is the spring torque. The spring returns the plate to a closed position when no armature voltage is applied. The spring assembly is initialized to an angle θ_0 such that T_{sp} is given by $T_{sp} = K_{sp}(\theta + \theta_0)$.

✓ T_a is a small torque induced by the airflow over the throttle plate which can be written as follows $T_a = R_{af} \cdot A_p \cdot \Delta P \cdot \cos^2 \theta$. where R_{af} is the distance from the throttle plate center to the force concentration point, $A_p = \pi R_p^2$ is the throttle plate area, $\Delta P = P_{atm} - P_m$ where P_m is the manifold pressure that is a nonlinear throttle angle dependent function, $P_m = f(\theta, P_{atm}, N)$ that approaches atmospheric pressure as the throttle approaches a wide-open state.

By taking $x = [\theta, d\theta/dt, i_a]^T$ as state vector and $u = e_a$ as input vector, ETC state representation becomes ($J = N^2 J_m + J_g$ and $K_f = (N^2 b_m + b_t)$):

$$\begin{aligned} \dot{x}_1 &= x_2 \\ \dot{x}_2 &= \frac{1}{J} \left(-K_{sp}(x_1 + \theta_0) - K_f x_2 + (NK_t)x_3 \right. \\ &\quad \left. - \pi R_p^2 R_{af} \Delta P \cdot \cos^2(x_1) \right) \\ \dot{x}_3 &= \frac{-1}{L_a} \left(NK_b x_2 + R_a x_3 + u \right) \end{aligned} \quad (2)$$

2.2 The ETC diagnosis problem

The ETC system is controlled in order to track some periodic reference signal θ_d . The corresponding control law may be designed for instance by exploiting the "triangular" structure of the equations (2) to derive a back-stepping based state feedback law (Krstic *et al.*, 1995). The underlying control used in the simulation hereafter is based on this methodology. The details are however skipped here since attention is concentrated on the **ETC** diagnosis problem. One has just to note that the diagnosis proposed in this paper is applied on the controlled system. This enables an on-line diagnosis to be achieved in order to monitor the parameters values during the system life-time. It is assumed that the angle $y = x_1 = \theta$ is measured by a rotational potentiometer sensor. The motor current i_a as well as the control input u are also assumed to be measured and can therefore be used in the diagnosis algorithm design. Therefore, the measurements vector $y_m \in \mathbb{R}^3$ is given by : $y_m := (x_1 \ x_3 \ u)$. The **ETC** diagnosis problem considered in the present paper may be stated as follows: Design an algorithm that uses the measurements vector to detect and isolate any even simultaneous variations in the parameter vector $(K_t \ R_a \ K_b \ K_f) \in \mathcal{K} \subset \mathbb{R}^4$ where \mathcal{K} is a domain of interest containing probable values of parameters.

3. DIAGNOSIS BY GRAPHICAL SIGNATURE

The starting point of this method is the known fact that "human eyes through the underlying brain activity" is able to accomplish high complexity classification tasks. This high classification ability needs however to be applied to some pattern. The aim of this method is to propose output-measurement-based generated patterns that are called signatures. More precisely a map from a high dimensional space to which belong the vector of past measurements over some moving time-window to \mathbb{R}^2 is defined. When applying this map to a moving-horizon past measurements, one obtains a bi-dimensional curve. Now, if for each faulty scenario, the "corresponding signature" differs from the nominal one in a distinguishably different way, from a human eye "viewpoint" then the graphical tool may be used in the context of fault detection and even isolation under certain assumptions. In order to clearly summarize the signature generation algorithm proposed in (Youssef and Alamir, 2003) and used hereafter to solve the **ETC** diagnosis problem, some definitions and notations are needed. This is the aim of the following section.

3.1 Some definitions and notations

The definitions given here refer to the case of one-dimensional output measurement. To this respect, each of the three components of y_m given above is used to generate a different signature.

3.1.1. The normalization function N_ε

Consider a scalar output y that is measured with some sampling rate. The vector of past measurements $y(t_1), \dots, y(t_N)$ is then used to construct a measurement vector Y . A normalization map is then applied to Y in order to obtain components that lie in $[-1, 1]$, namely

$$N_\varepsilon : \mathbb{R}^N \rightarrow \mathbb{R}^N ; N_\varepsilon(Y) = \bar{Y} = \frac{Y}{\|Y\|_\infty + \varepsilon} \quad (3)$$

where $\varepsilon > 0$ is some small regularizing coefficient while $\|Y\|_\infty$ is given by: $\|Y\|_\infty = \max|Y_i|_{i=1}^N$

3.1.2. Definition of a pencil P_ε

A pencil is a map $P_\varepsilon : \mathbb{R}^N \times \mathbb{R} \rightarrow \mathbb{R}^2$ that associates to each element (Y, y) of $\mathbb{R}^N \times \mathbb{R}$ (a set of $N + 1$ measurements) a point in the bi-dimensional plane:

$$P_\varepsilon : \mathbb{R}^N \times \mathbb{R} \rightarrow \mathbb{R}^2$$

$$(Y, y) \rightarrow \Phi_0(\bar{Y}) + \lambda_\varepsilon(\bar{Y}, y)[\Phi_1(\bar{Y}) - \Phi_0(\bar{Y})]$$

where:

$$\begin{aligned} \lambda_\varepsilon(\bar{Y}, y) &= \frac{y}{\|Y\|_\infty + \varepsilon} - \frac{1}{N} \sum_{i=1}^N \bar{Y}_i, \\ \Phi_0(\bar{Y}) &= \frac{1}{N} \sum_{j=1}^N \Psi_j(\bar{Y}); \Phi_1(\bar{Y}) = \frac{1}{N} \sum_{j=1}^N \bar{Y}_j \Psi_j(\bar{Y}), \\ \Psi_i(\bar{Y}) &= \frac{1}{2} [(1 + \bar{Y}_i) Q_{(i+1|N)} - (\bar{Y}_i - 1) Q_i] \\ Q_i &: \text{image}(e^{2j(i-1)\frac{\pi}{N}}) ; \quad j^2 = -1 \end{aligned}$$

$(Q_i)_{i=1}^N$ are the N nodes of a regular N -dimensional polygone in \mathbb{R}^2 , $(i + 1|N) = (i + 1) \text{Modulo } N$. $P_\varepsilon(Y, y)$ is a point on the line $\overrightarrow{\Phi_0 \Phi_1}$ with relative position defined by y . See (Youssef and Alamir, 2003) for more details.

3.2 Dynamical signature generation

Let us denote by δ the sampling time for measurements acquisition and define the following vector:

$$Y(t, N) = [y(t - N\delta), \dots, y(t - \delta)]^T \in \mathbb{R}^N \quad (4)$$

Using a moving window of width N from measurements $[y(t - i\delta)]_{i=0}^{m-1+N}$ and the pencil P_ε defined above, the following points in the 2D plane can be defined:

$$P_i(t, N) = P_\varepsilon \left(Y(t - (i - 1)\delta, N), y(t - (i - 1)\delta) \right) \quad i = 1 \dots m \quad (5)$$

$(P_i(t, N))_{i=1}^m$ define m points in R^2 which constitute the two-dimensional signature $S_\varepsilon(t, N)$ at time t . Analytically, $S_\varepsilon(t, N)$ can be written as follow: $S_\varepsilon(t, N) = (S_\varepsilon^x, S_\varepsilon^y)$ where $S_\varepsilon^x = (P_1^x(t, N) \dots P_m^x(t, N))^T$ and $S_\varepsilon^y = (P_1^y(t, N) \dots P_m^y(t, N))^T$. Note that Different signatures can be obtained by modifying the value of N which will be called signature order.

4. APPLICATION TO THE ETC DIAGNOSIS PROBLEM

In this section, the signature generation tool is used to solve the ETC diagnosis problem stated in section 2. The simulation parameters are listed in table 1. The throttle plate follows a sinusoidal reference signal of amplitude $0 \leq \theta \leq \frac{\pi}{2}$ and frequency $f = 0.17H$.

Tab. 1. Electronic throttle control system model parameter values.

Parameter	Value	Units	Parameter	Value	Units
b_m	0.03	$\frac{Nms}{rad}$	L_a	0.003	H
b_t	$3.397e^{-3}$	$\frac{Nms}{rad}$	N	4	-
L_g	0.005	kgm^2	P_{atm}	$1.01325e^5$	$\frac{N}{m^2}$
J_m	0.001	kgm^2	R_a	1.9	Ω
K_b	0.1051	$\frac{Vs}{rad}$	R_{af}	0.002	m
K_{sp}	0.4316	$\frac{Nm}{rad}$	R_p	0.0015	m
K_t	0.1045	$\frac{Nm}{A}$	θ_0	$\frac{\pi}{2}$	rad

Tab. 2. ETC system faults, domaine of variations of the parameters (\mathcal{K}).

No.	Description	Parameter	Interval
1	Motor torque coeff	K_t	[0.05 0.15]
2	Motor resistance	R_a	[1.5 2.5]
3	Back EMF	K_b	[0.05 0.15]
4	Throttle or Motor damping	K_f	[0.48 0.8]

According to the definition of the signature, one degree of freedom can be modified to be useful in diagnosis, namely, the signature order N . By taking 700 measurements of i_a , θ and u with a sampling period of $0.01s$ that is a moving window of $7s$, one generates four dynamical signatures: $S_1 = S_\varepsilon(t, 100)$ and $S_2 = S_\varepsilon(t, 200)$ (without normalisation, $\|Y\|_\infty = 1$) generated from i_a measurements, $S_3 = S_\varepsilon(t, 100)$ generated from θ measurements and $S_4 = S_\varepsilon(t, 50)$ generated from u measurements. Using this signatures, one could detect isolate and estimate all even simultaneous variations of the four considered parameters K_f , K_t , R_a and K_b within the prescribed regions given in table 2. As it is shown in the following section, ETC diagnosis is done in the following order: K_f , K_t , R_a and then K_b .

4.1 Detection of variations on K_f

The allure of the signature S_1 in the case of variations affecting K_f under nominal values of (K_t, R_a, K_b) is illustrated on figure 2. It is easy to notice that when K_f increases, the allure of the signature S_1 lengthens. Now, the interesting question is: How does this property (residual) changes when the other parameters vary ?

Figures 3,4, 5 show that the signature S_1 is insensitive to variations on the other parameters, thus one can use this signature to detect, isolate and estimate variations on K_f without knowing the other parameters. Note that interesting points of S_1 are clearly those corresponding to minimal values for y-coordinate. Consequently the mathematical, say residual r_{kf} which allows us to detect, isolate and estimate variations on K_f can be written as follow: $r_{kf}(t) = \min[S_1^y]$.

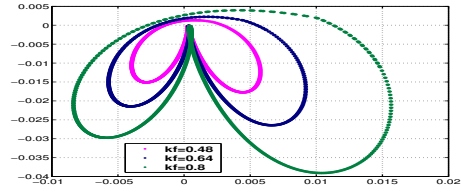


Fig. 2. Sensitivity of the signature S_1 to variations on K_f , $(K_t, R_a, K_b) = (0.1045, 1.9, 0.1051)$.

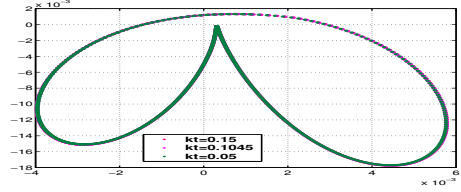


Fig. 3. The signature S_1 is insensitive to variations on K_t , $(K_f, R_a, K_b) = (0.48, 1.9, 0.1051)$.

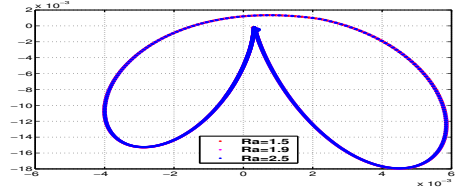


Fig. 4. The signature S_1 is insensitive to variations on R_a , $(K_f, K_t, K_b) = (0.48, 0.1045, 0.1051)$.

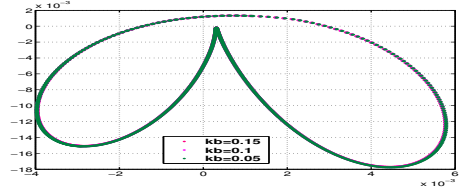


Fig. 5. The signature S_1 is insensitive to variations on K_b , $(K_f, K_t, R_a) = (0.48, 0.1045, 1.9)$.

4.2 Detection of variations on K_t

The allure of the signature S_2 in the case of variations affecting K_t under nominal values of (K_f, R_a, K_b) is illustrated on figure 6. It is clear that when K_t decreases, the allure of the signature S_2 lengthens. Like the previous case, interesting points of S_2 are those corresponding to minimal values for y-coordinate and consequently K_t -estimation can be done using this points. Note that this property of S_2 remains valid for all admissible values of K_f and this signature is insensitive to variations on R_a and K_b (see figures 7,8). Thus one can use this signature to detect, isolate and estimate variations on K_t if the value of K_f is known and without knowing the value of (R_a, K_b) . Note that the value of K_f can be estimated by using the signature S_1 . Consequently, residual r_{kt} which allows us to detect, isolate and estimate variations on K_t can be written as follow: $r_{kt}(t) = \min[S_2^y]$.

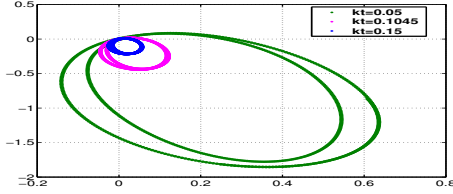


Fig. 6. Sensitivity of the signature S_2 to variations on K_t , $(K_f, R_a, K_b) = (0.48, 1.9, 0.1051)$.

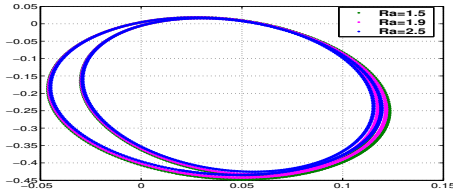


Fig. 7. The signature S_2 is insensitive to variations on R_a , $(K_f, K_t, K_b) = (0.48, 0.1045, 0.1051)$.

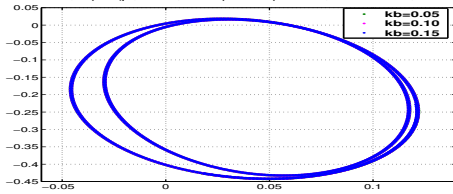


Fig. 8. The signature S_2 is insensitive to variations on K_b , $(K_f, K_t, R_a) = (0.48, 0.1045, 1.9)$.

4.3 Detection of variations on R_a

Figure 9 illustrates the allure of the signature S_3 in the case of variations affecting R_a under nominal values of (K_f, K_t, K_b) . It is easy to notice that when R_a increases, the right point of the signature S_3 shift to the right. In this case, Interesting points which allow us the estimation of R_a are those of S_3 corresponding to maximal values for x-coordinate. Note that this property of S_3 remains

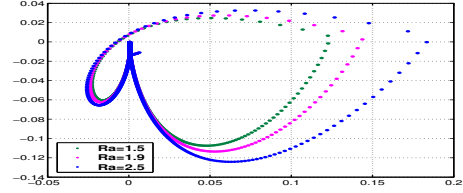


Fig. 9. Sensitivity of the signature S_3 to variations on R_a , $(K_f, K_t, K_b) = (0.48, 0.1045, 0.1051)$.

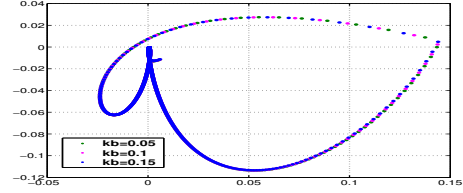


Fig. 10. The signature S_3 is insensitive to variations on K_b , $(K_f, K_t, R_a) = (0.48, 0.1045, 1.9)$.

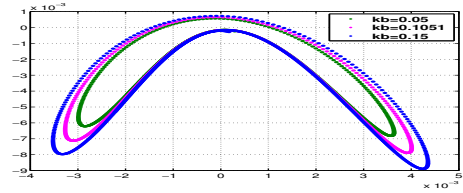


Fig. 11. Sensitivity of the signature S_4 to variations on K_b , $(K_f, K_t, R_a) = (0.48, 0.1045, 1.9)$.

valid for all admissible values of (K_f, K_t) and this signature is insensitive to variations on K_b (see figure 10). Thus one can use this signature to detect, isolate and estimate variations on R_a if the value of (K_f, K_t) is known and without knowing the value of K_b . (K_f, K_t) can be estimated using the signatures S_1 and S_2 . Consequently residual r_{ra} which allows us to detect, isolate and estimate variations on R_a can be written as follow: $r_{ra}(t) = \max[S_3^x]$.

4.4 Detection of variations on K_b

Figure 11 illustrates the allure of the signature S_4 in the case of variations affecting K_b under nominal values of (K_f, K_t, R_a) . It is easy to notice that when K_b increases, the allure of the signature S_4 lengthens. Interesting points of S_4 are those corresponding to minimal values for y-coordinate and consequently K_b -estimation can be done using this points. Note that this property of S_4 remains valid for all admissible values of (K_f, K_t, R_a) . Thus one can use this signature to detect, isolate and estimate variations on K_b if the value of (K_f, K_t, R_a) is known. (K_f, K_t, R_a) can be estimated using the signatures S_1 , S_2 and S_3 associated to the above sections. Consequently residual r_{kb} which allows us to detect, isolate and estimate variations on K_b can be written as follow: $r_{kb}(t) = \min[S_4^y]$.

5. ETC PARAMETERS ESTIMATION

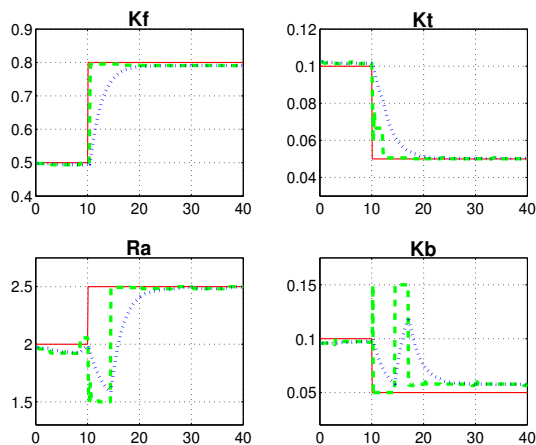


Fig. 12. On line ETC estimated parameters in the case of simultaneous change at $t=10s$ (real parameters: solide line '-', estimated parameters: dashed line '- -', estimated parameters after filtering: dotted line'·').

Based on the mathematical residuals defined above, the on-line ETC parameters estimation can be done by cubic interpolation method. Parameters estimation is done in the following order: K_f , K_t , R_a and then K_b . For instance the estimated R_a given \hat{K}_f , \hat{K}_t is the solution of $\varphi(R_a) = measured [r_{ra}(t)]$ where $\varphi(\sigma)$ is the residual $r_{ra}(t)$ computed with $K_f = \hat{K}_f$, $K_t = \hat{K}_t$ and $R_a = \sigma$. Figure 12 shows estimated parameters in the case of simultaneous parameters change from $[K_f = 0.5, K_t = 0.1, R_a = 2, K_b = 0.1]$ to $[K_f = 0.8, K_t = 0.05, R_a = 2.5, K_b = 0.05]$ at $t=10s$. A white noise is added to measurements (see figure 13). Since all signatures and residuals are defined for a constant values of the parameters in a moving window of width $L = 7s$, signatures generated by a measurement window containing the step change are not relevant. For this reason estimated parameters are filtered by a low pass filter with cut-off frequency $f_0 = 1/L$.

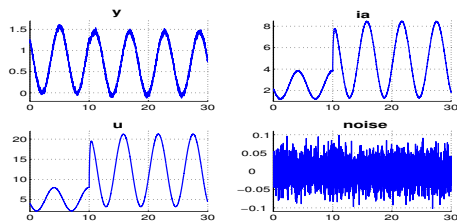


Fig. 13. Measurements with simultaneous parameters change at $t=10s$.

6. CONCLUSION

In this paper, automotive electronic throttle systems diagnosis based on graphical signature tool is

proposed. This graphical tool when joined to the particularly powerful human classification ability facilitates the extraction of relevant graphical residuals. The latter can then be expressed in a mathematical form for use in a real time context. Representative numerical results are presented and discussed to demonstrate the performance of the graphical signature tool in diagnosing a suite of ETC system failures. On line parameters estimation are presented.

REFERENCES

- Basseville, Michèle. (1998). On-board component fault detection and isolation using the statistical local approach.. *Automatica* **34**(11), 1391–1415.
- Conatser, R. and J. Wagner (2000). Health monitoring for automotive electronic throttle control systems.. In: *Proceedings of the seventh mechatronics forum international conference*. Atlanta, GA. pp. 135–159.
- Conatser, R., J. Wagner, S. Ganta and I. Walker (2004). Diagnosis of automotive electronic throttle control systems.. *Control Engineering Practice*. **12**(1), 23–30.
- Ding, X. and L. Guo (1998). An approach to time domain optimization of observer-based fault detection systems.. *Int. J. Control* **69**(3), 419–442.
- Huber, Lieberoth-Leden, Maisch and Reppich (1991). Electronic throttle control.. *Automotive Engineering*. **99**(6), 15–18.
- Krishnaswami, V., G. C. Luh and G. Rizzoni (1995). Nonlinear parity equation based residual generation for diagnosis of automotive engine faults.. *Control Engineering Practice*. **3**(10), 1385–1392.
- Kristicacute, M., I. Kanellakoupoulos and P. V. Kokotovic (1995). *Nonlinear and adaptive Control design*. Control System Technology and Automation. Wiley.
- Petropol, S. (2001). Ondelettes et diagnostic, application aux défauts diélectriques et électriques des machines tournantes. PhD thesis. INPG. Grenoble, France.
- Staroswiecki, M. and G. Comtet-Varga (2001). Analytical redundancy relations for fault detection and isolation in algebraic dynamic systems.. *Automatica* **37**(5), 687–699.
- Xiang-Fang, Sun, Fan Yue-Zu and Zhang Fei-Zhou (2002). Fault detection using an adaptive fuzzy system.. *Int. J. Syst. Sci.* **33**(7), 599–609.
- Youssef, B. and M. Alamir (2003). Generic signature generation tool for diagnosis and parametric estimation of multi-variable dynamical nonlinear systems. In: *Proceedings of the IEEE Conference on Decision and Control, Hawaii, USA*.